Estimation of the Dust Mass with Infrared Emission and Extinction of Supernova Remnants: G156.2+5.7, G109.1-1.0, G166.0+4.3, G93.7-0.2

Zhe Zhang(张哲), Biwei Jiang(姜碧沩), Jun Li(李军) and He Zhao(赵赫)

BACKGROUND

The violent explosions of supernovae provide vast amounts of dust to the interstellar medium(ISM). As they produce dust, they also destroy the surrounding interstellar medium. Therefore, the determination of the mass of supernova remnant(SNR) dust is an important content. There are two ways to estimate the SNR's mass. Firstly, the mass of SNR can be estimated by fitting the observational spectral energy distribution(SED) by the existing dust model. Second, the mass of SNR can also be estimated by constructing 3D extinction maps. The advantages and disadvantages of the two methods can be complementary, so the mass of SNR can be estimated and the results of two ways can be compared.

DATA

The data of Infrared images

- **WISE**
  3.4, 4.6, 12, 22 (μm)
- **AKARI**
  65, 90, 140, 160 (μm)
- **IRAS**
  12, 25, 60, 100 (μm)
- **Planck**
  350, 550, 850, 1380 (μm)

Circle of SNR & background annulus

- **G156.2+5.7**
  center/inner/outer circle radii: 63′, 76.8′, 94.8′
- **G109.1-1.0**
  center/inner/outer circle radii: 18.6′, 21.6′, 27.6′
- **G93.7-0.2**
  center/inner/outer circle radii: 40.2′, 48′, 60.6′
- **G166.0+4.3**
  center/inner/outer ellipses width & height:
  81′ & 51′; 95.4′ & 60′; 114.6′ & 72′

The data of Extinction:
The dust maps are retrieved by the **BayestarQuery** function in the Python package dustmaps.

Dust Mass Derived from the Infrared Emission

The example in multiband images

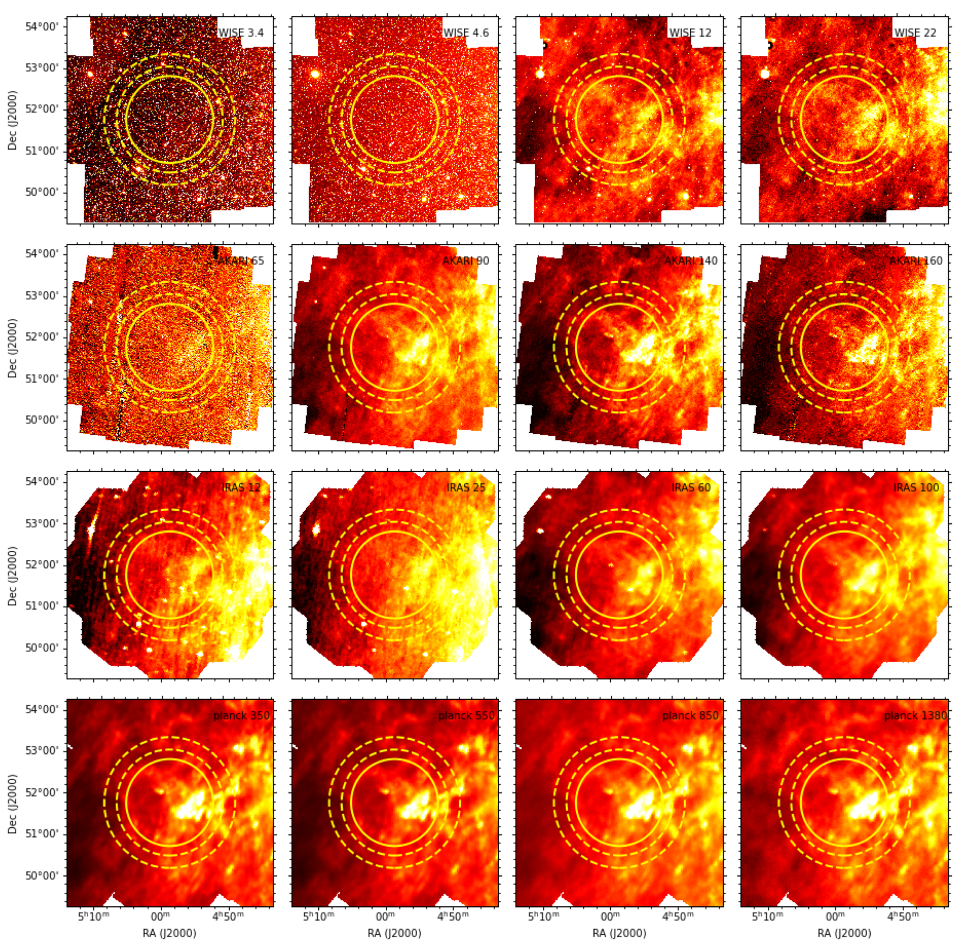

Figure 1: The multiband images of **G156.2+5.7** at R.A. = $04^h58^m40^s, +51^{\circ}50'00''$ in the WISE(first low), AKARI(second raw), IRAS(third raw), Planck(fourth raw). The yellow solid circle marks the center with a radius of 63', and the yellow dashed circles indicate the background annulus with inner and outer radii of 76.8' and 94.8' respectively. Each image is displayed at its original resolution and pixel size.

Method of Infrared Emission

$$F_\nu(\lambda) = \frac{M_w}{D^2}\kappa(a,\lambda)B_\nu(\lambda,T_w) + \frac{M_c}{D^2}\kappa(a,\lambda)B_\nu(\lambda,T_c)$$

1. M_w : mass of the warm dust
2. M_c : mass of the cold dust
3. D: *distance*
4. $\kappa(a,\lambda)$: mass absorption coefficient $\quad \kappa(\lambda) = \kappa_{\lambda_0}\left(\frac{\lambda_0}{\lambda}\right)^\beta$
5. $B_\nu(\lambda,T)$: Planck function

a: grain radius
When grain size < 1 μm at wavelengths longer than 10 μm, the for both silicate and graphite is nearly independent.
κ_{λ_0}: the κ value at reference wavelength λ_0
β: the dust emissivity index

λ_0: **500 μm** $\quad \kappa_{\lambda_0}$: **1.45 cm^{2}g^{-1}** $\quad \beta = 2.04$

The mass and temperature of SNRs

	G109.1-1.0	G156.2+5.7	G166.0+4.3	G93.7-0.2
$M_w(M_\odot)$	$0.04^{+0.007}_{-0.006}$	$0.002^{+0.0004}_{-0.0003}$	$0.05^{+0.01}_{-0.01}$	$0.01^{+0.005}_{-0.004}$
T_w(K)	$60.1^{+1.2}_{-1.0}$	$64.1^{+1.2}_{-1.1}$	$42.7^{+0.62}_{-0.62}$	$68.4^{+4.2}_{-3.2}$
$M_c(M_\odot)$	$100.8^{+9.1}_{-8.3}$	$151.9^{+3.8}_{-3.4}$	$75.3^{+7.5}_{-7.4}$	$446.1^{+17.6}_{-17.7}$
T_c(K)	$16.1^{+0.31}_{-0.3}$	$13.2^{+0.12}_{-0.13}$	$12.9^{+0.28}_{-0.29}$	$14.7^{+0.14}_{-0.14}$

Results of SED of four SNRs

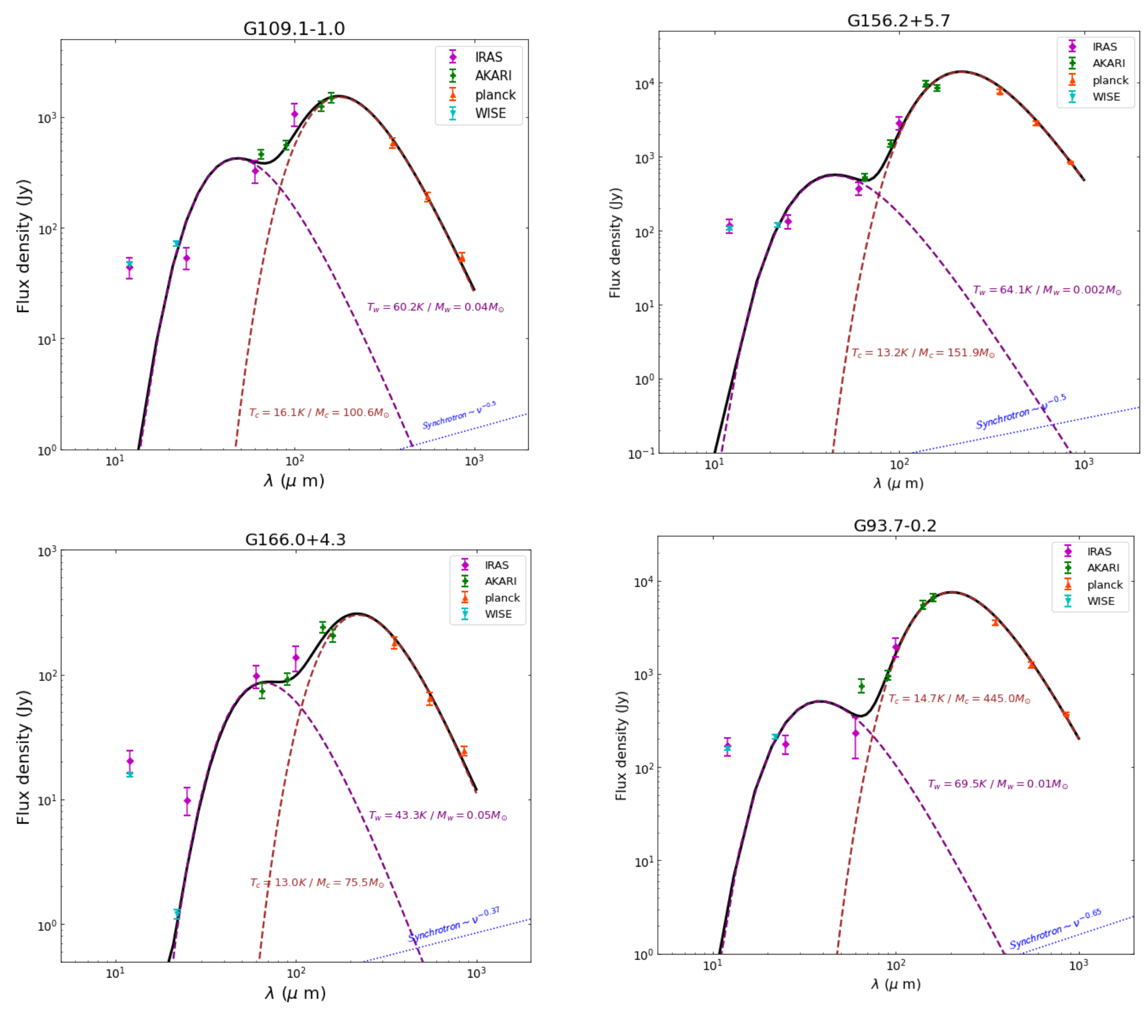

Figure 2: The **SED fitting** of G109.1-1.0, G156.2+5.7, G166.0+4.3 and G93.7-0.2 with measurements by WISE, AKARI, IRAS and Planck. The black solid line represents the sum of two dust components and synchrotron emission (bule dotted line), the best fitted warm and cold dust components are shown by pink and brown dashed lines, respectively.

Dust Mass Derived from the Extinction

Extinction jumps

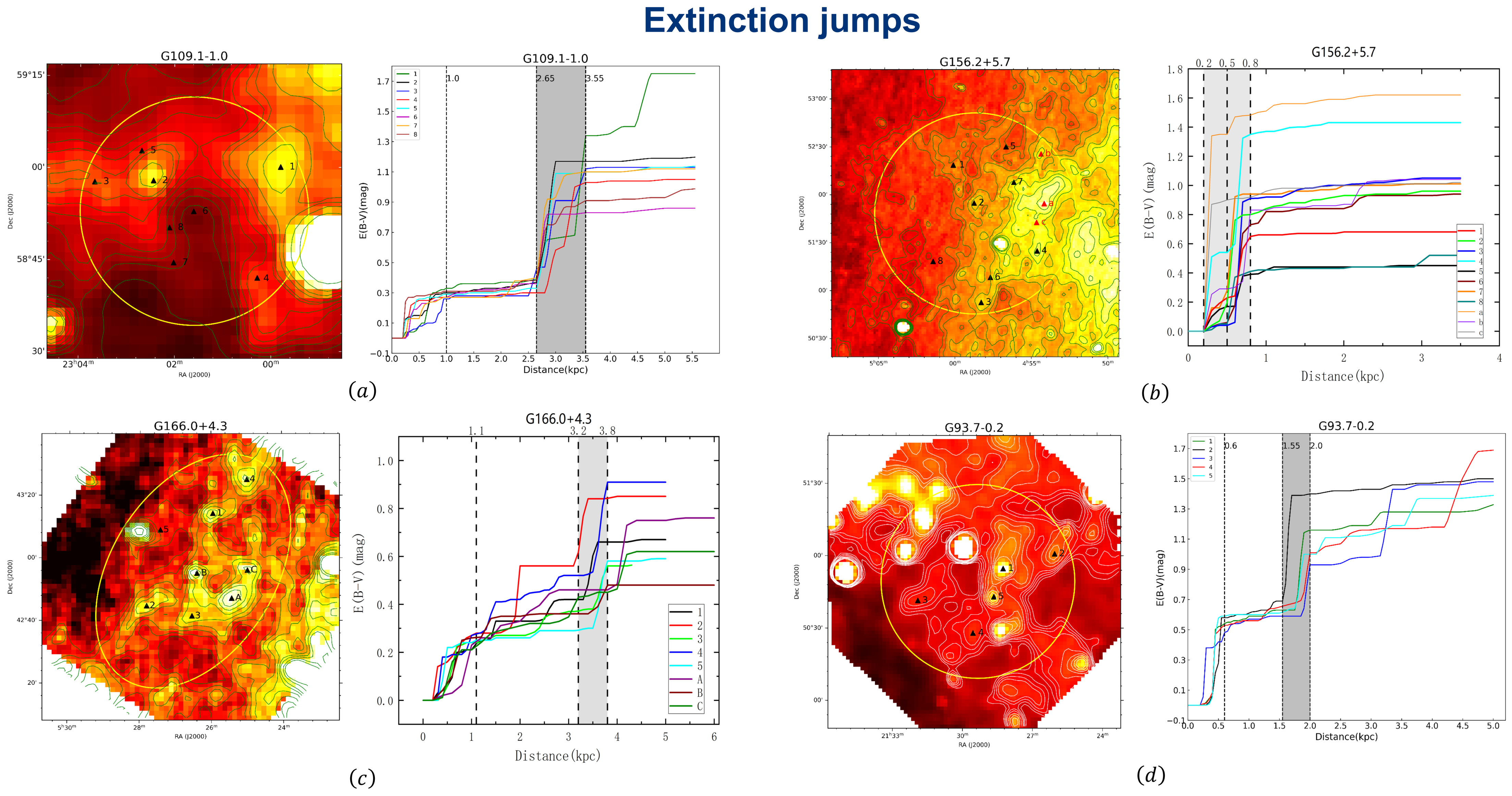

Figure 3: The infrared images in the IRAS 25 μm and color excess *E(B-V)* vs distance images of G109.1-1.0 (a), G156.2+5.7 (b), G166.0+4.3 (c), G93.7-0.2 (d). The distance is extracted from the 3D extinction map of Green et al (2018). The images of the four SNRs are overlaid with the contours of the 25 μm images, and the yellow solid circles/ellipses indicate the photometry aperture at the respective sizes of the SNRs. Clump points are marked with black triangles in the images. The lines in various colors correspond to those markers in the infrared images. The vertical gray areas indicate the extinction jumps toward the SNRs within the distance range.

Method of Extinction

$$M_d^{\rm ext} = \sum_{\rm dust} \times A_{\rm SNR} = \frac{A_V}{K_V^{\rm ext}} \times A_{\rm SNR}$$

1. $K_V^{\rm ext}$: mass extinction coefficient for V band
   $K_V^{\rm ext} = 3.7^{+0.5}_{-0.8} \times 10^4$ mag/(g cm^{-2})
2. $A_{\rm SNR}$: area of SNR
3. $A_V = 2.742 \times E(B-V)$

The area of the SNR is calculated with the distance listed in the Table below, and the aperture size showed with yellow circle/ellipse in Figure 3.

Results

The extinction distance/average A_V/mass of SNRs

	G109.1-1.0	G156.2+5.7	G166.0+4.3	G93.7-0.2
distance (kpc)	2.8	0.68	3.2	2.0
average A_V (mag)	1.2	1.9	0.3	0.6
$M_{\rm ext}(M_\odot)$	$108.8^{+28.2}_{-13.6}$	$117.8^{+30.7}_{-14.6}$	$93.7^{+25.3}_{-12.0}$	$123.6^{+32}_{-15.4}$

SUMMARY

- The dust mass is estimated to be about 101 $M_\odot$(G109.1-1.0), 152 $M_\odot$(G156.2+5.7), 77 $M_\odot$(G166.0+4.3) and 445 $M_\odot$(G93.7-0.2), from fitting the spectral energy distribution in the infrared bands observed by WISE, IRAS, AKARI, and Planck.
- The extinction caused by the SNR is determined by identifying the extinction jump in the correct distance range.
- The dust mass is estimated approximately 109 $M_\odot$(G109.1-1.0), 118 $M_\odot$(G156.2+5.7), 94 $M_\odot$(G166.0+4.3) and 124 $M_\odot$(G93.7-0.2) with the help of the extinction maps provided by the Bayestar.
- The dust mass from infrared emission is different from that from extinction in the same SNR. Therefore, reliable results require a comparison of both methods.

REFERENCES

1 Green, G. 2018, JOSS, 3, 695
2 Li, J., Jiang, B., & Zhao, H. 2022, ApJ, 927, 226
3 Wang, S., Zhang, C., Jiang, B., et al. 2020, A&A, 639, A72
4 Zhao, H., Jiang, B., Gao, S., Li, J., & Sun, M. 2018, ApJ, 855, 12
5 Zhao, H., Jiang, B., Li, J., et al. 2020, ApJ, 891, 137